

# Experimental Study on Mechanical Properties of Lightweight Concrete with Shale Aggregate Replaced Partially by Nature Sand

X.G. Zhang, X.M. Kuang, J.H. Yang

School of Civil Engineering, Henan Polytechnic University, Jiaozuo 454003, China

S.R. Wang\*

International Joint Research Laboratory of Henan Province for Underground Space Development and Disaster Prevention, Henan Polytechnic University, Jiaozuo 454003, China

[w\\_sr88@163.com](mailto:w_sr88@163.com)

**ABSTRACT:** To study the basic mechanical properties of lightweight concrete incorporating shale aggregate replaced partially by nature sand (LCSARP), a variety of mixes were designed and the properties of the mixes were determined through a series of laboratory tests including compressive strength test, splitting tensile strength test, flexural strength test and tests to determine modulus of elasticity and poisson's ratio. The failure processes, failure modes and the influences of replacement rate of natural sand on essential mechanical properties of LCSARP were studied. The result show that the failure modes of LCSARP are different from ordinary Portland cement concrete. In General, the mechanical properties of LCSARP show an increasing trend with the incremental replacement rate of natural sand, including  $f_{cu}$ ,  $f_c$ , splitting tensile strength, flexural strength,  $f_c/f_{cu}$ , tension and compression's ratio, and the ratio (defined as similar flexure and compression's ratio (SFCR)) between flexural strength and the square root of cube compressive strength. With the incremental replacement rate of natural sand, the elastic modulus of LCSARP increases gradually, while the reverse is true for the Poisson's ratio. In terms of LCSARP, a precise and applicable relationship for the mechanical property parameter as  $f_{cu}$ ,  $f_c$ , splitting tensile strength, flexural strength,  $f_c/f_{cu}$  at different replacement rates of natural sand was individually established by the regression analysis. A parabolic function between tension-to-compression ratio and Poisson's ratio for LCSARP was established that correlates well to the experimentally measured results.

## 1 INTRODUCTION

Lightweight concrete is characterized by the use of consists of natural porous lightweight aggregate or artificial ceramsite particles as coarse aggregates, natural (normal) sand or lightweight sand as fine aggregates [1-2]. The dry density of lightweight aggregate concrete is typically less than  $1950 \text{ kg/m}^3$ , of which the mechanical and thermal properties varies with its density. Due to the advantages of lightweight, good thermal insulation and durability, lightweight aggregate concrete is widely used in high rise structures, marine structures and bridges [3-4]. Compared with ordinary concrete, lightweight aggregate concrete can reduce the self-weight of the structure by 20% - 40% while maintain the same moment capacity, which is beneficial to the performance of the structure, and especially to the seismic performance [5]. As one type of lightweight aggregate concretes, the coarse and fine aggregates of All Light Concrete (ALC) are both light weight, so compared with ordinary lightweight aggregate concrete, the most outstanding advantage of ALC is lighter and better thermal insulation. However, there are disadvantages associated with ALC such as higher cost,

poor working performance and high requirements for production of lightweight aggregate, which had seriously limited its application in engineering structures [6-7].

LCSARP can be obtained through ALC by partly or completely replace lightweight sand by normal sand [8]. The natural sand is convenient to take raw material and cost-effective. Due to the high self-weight of natural sand and interface friction caused by large contact area between natural sand of small particle size and lightweight aggregate, floating in construction and blocking in pumping for lightweight aggregate can be solved to some extent [9]. In addition, because of packing effect of natural sand, the compactness of LCSARP is enhanced significantly [10]. LCSARP can mitigate the problems with ALC in terms of mechanical properties, high cost and construction issues. Therefore, it is necessary to carry out the further and systematic research on the preparation and performance of LCSARP [11-12].

## 2 STATE OF THE ART

Previous research results mainly focused on concrete that consists of lightweight coarse aggregate, natural sand or lightweight sand. On the preparation of lightweight aggregate concrete, lightweight aggregate concrete has been prepared with high water cement ratio by Chen et al. [26], which significantly reduces the slump loss and the floatation level of light aggregate, while ensures the high strength. Li et al. [14] based on the MFT (Packing and Mortar Film Thickness) theory, proposed an effective mix proportion design method for self-compacting lightweight concrete. El-Hassan et al. [15] developed a dynamic curing system of carbon dioxide to significantly improve the early and late strength of lightweight aggregate concrete. The lightweight coal bottom ash aggregate concrete was prepared successfully by Kim et al. [16], and its 28d compressive strength reached 22.7-27.8 MPa. Regarding mechanical properties of lightweight aggregate concrete, dynamic constitutive model of alumina bubble-basalt fiber lightweight aggregate concrete was constructed by Ye [17], and their stress-strain model relates well to that measured. Kockal et al. [18] studied the influence of aggregate type on the mechanical properties of lightweight concrete, the results showed that lightweight aggregate could reduce the strength of concrete, and an ideal slump and gas content could be achieved by adding a small amount of chemical admixtures. Oktay et al. [19] studied the mechanical properties of lightweight aggregate concrete mixed with pumice, expanded perlite and rubber particles, which reduced the compressive strength of concrete, but still met the requirements of specification. Davraz et al. [20] measured the mechanical properties of artificial lightweight aggregate concrete, including compressive strength, elastic modulus and Poisson's ratio, and established the estimation model of elastic modulus and Poisson's ratio.

On the durability of lightweight aggregate concrete, Li et al. [21] showed that the durability of such concrete design could be improve significantly the durability of high performance lightweight aggregate concrete by adding moderate amount of fly ash, mineral powder or silica fume and other mineral admixtures. Kockal [22] studied the durability of fly ash lightweight aggregate concrete, the results showed that the resistance to water penetration and chloride ion penetration of fly ash lightweight aggregate concrete is slightly lower than ordinary concrete, but it had good anti-freeze-thaw cycle performance. Demirboga et al. [23] studied anti-freeze-thaw cycle performance of lightweight expanded perlite and pumice aggregate concrete with the addition of silica fume and fly ash and perlite at the same time, the results showed that the anti-freeze-thaw cycle

performance of lightweight aggregate concrete could be increased by 1.30, 0.83, and 0.18 times, with adding expanded perlite, fly ash and silica fume, respectively. Rossignolo et al. [24] studied the durability of SBR (Styrene-butadiene Rubber Latex) modified lightweight aggregate concrete, the results showed that the water absorption was reduced and the corrosion resistance was improved significantly by SBR. On the theoretical model of lightweight aggregate concrete, Wang et al. [25] proposed a unified model to accurately predict the compressive strength and shrinkage of lightweight aggregate concrete as considering the volume ratio and water content of pre-wet aggregate. Yaseen et al. [26] proposed a high precision ELM (Extreme Learning Machine) model to predict the compressive strength of lightweight foam concrete.

It can be found from the current research that previous researches primarily focus on the preparation, static and dynamic performance, durability performance and theoretical model of lightweight aggregate concrete, which played a role in further promoting the application and practice of lightweight aggregate concrete. However, the research is seldom reported on the mechanical properties of LCSARP so far. Qiant al. [27] prepared the LCSARP with crushed stone, fly ash, shale pottery and river sand, an ideal lightweight and high strength was achieved, and the thermal insulation properties of LCSARP could be improved significantly by mixing an appropriate amount of natural sand.

Natural sand was employed to replace the shale pottery in all light concrete in this paper, its basic mechanical properties were tested, the failure process and failure mode of LCSARP were analyzed, the relationship between mechanical properties indexes and natural sand replacement rate was proposed. Finally, the law between Poisson's ratio and tension and compression's ratio was studied. It is expected to provide reference for further research and engineering application of LCSARP.

## 3 MATERIALS AND METHOD

### 3.1 Raw materials for the experiment

The normal Portland cement (P·O 42.5 MPa) was sourced from Jiaozuo, China. The blending water was ordinary water. The physical properties of lightweight aggregate produced by a company at Luoyang, China were listed as followed: lightweight coarse aggregate of grade 700 crushed shale ceramsite with particle size less than 15 mm, cylindrical compress strength of 4.5 MPa, and bulk density of 660 kg/m<sup>3</sup>, lightweight fine aggregate of grade 900 shale pottery with particle size less than 5 mm, bulk density of 880 kg/m<sup>3</sup>, and fineness modulus of 3.15.

The characteristics of river sand are the following measured properties: particle sizes of less than 5 mm, bulk density of 1472 kg/m<sup>3</sup>, fineness modulus of 2.85, and continuous grading.

### 3.2 Mix proportion design

With shale ceramsite as coarse aggregate and shale pottery replaced by natural sand in fine aggregate, five replacement rates of LCSARP specimens were prepared, in which all light concrete specimens with the replacement rate of 0% was taken as the reference specimen, and other four different volume contents of shale ceramsite were taken as a testing specimen, including 25%, 50%, 75% and 100%. Before

experiment, the materials were processed with the following procedure: (1) Presoaking the bagged ceramsite for 12 hours. (2) Taking out the ceramsite before stirring, and letting the water lost from the ceramsite until reaches a constant weight. (3) Mixing with other raw materials in accordance to the mixing proportion. Fly ash accounted for 33.7% of cement. The water reducing ratio of polycarboxylate superplasticizer was greater than 20%, and it accounted for 1.0% of cementitious material dosage. Based on the mixing proportion of LC35 all light concrete strength, the LCSARP with different replacement rates were adjusted in according to the mixing proportions in Table 1.

Table 1. Mixing proportion of LCSARP (kg/m<sup>3</sup>)

Number	$\gamma$ /%	Cement	Water	Ceramic granule	Shale pottery	Nature sand	Fly ash	Water reducer
2-0	0	472	171	444	408	0	159	6.31
2-1	25	472	171	444	306	170	159	6.31
2-2	50	472	171	444	204	341	159	6.31
2-3	75	472	171	444	102	512	159	6.31
2-4	100	472	171	444	0	682	159	6.31

Note:  $\gamma$  is the replacement rate of natural sand; Numbers 2-0, 2-1, 2-2, 2-3 and 2-4 represent specimens with the natural sand replacement rate of 0 %, 25 %, 50 %, 75 % and 100 %, respectively.

### 3.3 Test sample preparing and loading method

The cube specimens of 150 mm × 150 mm × 150 mm and the prism specimens of 150 mm × 150 mm × 300 mm and 150 mm × 150 mm × 550 mm were adopted. Each strength experiment was designed for 5 groups of 3 blocks in each group, with a total of 60 blocks. Following Chinese standard specification GB/T 50080-2002 [28], the standard plastic moulds were adopted to mold concrete, which were removed after 24 hours, and then the specimens were cured for 28d at room temperature before measuring the strength. The longitudinal and transverse strain gages were attached to the side of the axial compression prism which were then graded and loaded to obtain the load-longitudinal (transverse) strain curve.

Testing was performed in accordance with the Chinese standard specification GB/T 50081-2002 [29], the SYE-1000-type pressure testing machine with the maximum range of 1000 kN was used as loading device.

## 4 RESULTS AND DISCUSSION

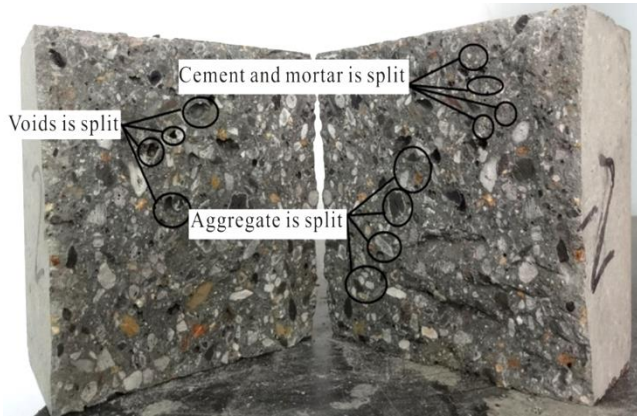
### 4.1 Failure process and failure mode

Figure 1 shows the failure mode of each group specimen under cube compression. At the initial stage of loading, no cracks appeared on the surface of

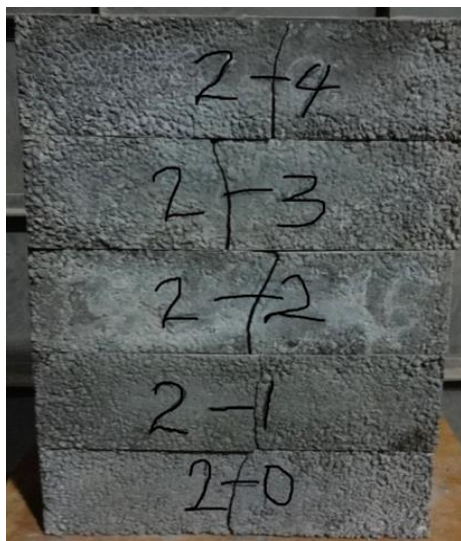
specimens. As the load increased, internal stress of LCSARP increased and the micro cracks appeared at the flank of specimens in the case of vertical compression and horizontal free expansion. As the load further increased, specimens were destroyed when the adjacent cracks were connected and specimen's flank was outer drums. The specimens produced a sharp crackle when failure was near, and 2-3 cracks developed rapidly, and the ceramsites were ejected from the concreting surface. The internal structure of LCSARP is different from the ordinary concrete, which results in different failure mode. It can be observed from Figure 1 that the brittleness of LCSARP is more remarkable when the replacement rate of natural sand is less than or equal to 25% after the failure, and cracking and spalling of concrete are more serious in the specimen's flank after the failure, especially the edge-sides of specimens. However, as the replacement rate of natural sand is greater than 25 %, the failure mode of LCSARP is characterized by fracture and less obvious burst, and without scattering. Therefore, compared with the all light concrete, the brittleness of LCSARP decreases gradually as the replacement rate of natural sand increases, but its toughness increases in a contrary direction.



a) Cube compressive test      b) Axial compressive test



c) Splitting tensile test



d) Flexural strength test

Figure 1. The failure modes of the samples

Figure 1(b) shows the failure mode of each group specimen under axial compression. At the initial stage of loading, no cracks appeared on the surface of specimens. When the load approached to the peak load, cracking of aggregate could be heard, and the axial compression of prism specimens appeared earlier than the cube specimens. It could be observed that the surface cracks of specimen expanded rapidly, the concrete was spalled continuously at the specimens' flank, and then the specimens damaged. From Figure 1(b), it can be observed that the failure is characterized by longitudinal splitting, as the replacement rate

of natural sand is less than or equal to 50%. The reason for cracks is that lightweight aggregate don't have enough strength to stop the increasing load in LCSARP. As the load increasing continuously, the adjacent cracks are penetrated, and the prism specimens split into a number of separate small prisms, then the specimens are damaged due to inadequate bearing capacity in general. With the replacement rate increasing from 75% to 100%, specimen bearing capacity increases and prism specimens generate a wider main crack in the direction of 45°, the central concrete spalls, and the failure mode becomes the shear failure of oblique section.

In general, the failure mode of LCSARP is basically similar to all light concrete under the experiment of splitting tensile. At the initial stage of loading, no cracks appeared on the surface of specimens. As the load increasing, the initial micro cracks generated at the specimens' shear flank. When the ultimate tensile load was reached, cracks were penetrated quickly, the specimens were split into two parts and damaged with a bang. From Figure 1(c), it can be viewed that the failure sections of specimens are different from the ordinary concrete, the damage consists of three parts: (1) voids are split, (2) cement and mortar is split, (3) ceramsite and shale pottery are split, in which the (3) plays a major role. Its section structure is level and homogeneous for subjecting to splitting failure, and there is no separated phenomenon that ceramsite floats and cement mortar submerges in the failure surface. The damage of the specimens can be attributed to brittle failure with obvious crack.

At the initial stage of loading, it showed no obvious cracks in the specimen's flank under the flexural experiment. As the load further increased, stress increased in concrete, which caused the initial micro cracks in the middle of tension surface, then cracks were widen and developed to the compression side. At last, a loud thump appeared and the specimens were split into two parts. The failure process developed rapidly from cracks to rupturing into two parts, which can be attributed to brittle failure. From Figure 1(d), it is shown that there is no vertical development for the main crack and no a standard for the crack development under different replacement rates. The main reason is that the fracture resistance of LCSARP is more sensitive to the crack of the tensile surface, there is no obvious law in the distribution for ceramsite and shale pottery in concrete, and the strength is lower than cement paste, namely, the strength of LCSARP is restricted by lightweight aggregate with low strength. Therefore, once the load increases to a certain extent, lightweight aggregate will become a weak link of failure, and cracks will develop rapidly along the weak links.

4.2 Mechanical properties and influence factors

The multi-stage loading were taken to obtain the upward section curve for axial load-strain and the lateral load-strain in this experiment, the ratio of stress and strain is used as elastic modulus at the  $0.4 f_c$  of upward section of axial load-strain curve, Poisson's ratio is the average value of the ratio of lateral strain and axial strain. The mechanical performance indexes of

LCSARP are listed in Table 2. It can be found from Table 2 that the cube compressive strength of all light concrete has reached 35.8 MPa, which meets the design requirements of LC35 grade. With the incremental replacement rate of natural sand, the compressive strength of LCSARP increases gradually, the strength grade of LCSARP with 100% nature sand is LC40 at least.

Table 2. Mechanical property test results of LCSARP

Number	$\gamma$ /%	$f_{cu}$ /MPa	$f_c$ /MPa	$f_{ts}$ /MPa	$f_f$ /MPa	$f_c / f_{cu}$	$f_{ts} / f_{cu}$	$f_f / f_{cu}$	SFCR	$E_c$ /GPa	$\nu$
2-0	0	35.8	24.7	3.13	6.10	0.69	0.087	0.170	1.02	22.06	0.28
2-1	25	40.0	33.7	3.45	6.25	0.84	0.086	0.156	0.99	22.17	0.18
2-2	50	42.1	35.9	3.76	6.75	0.85	0.089	0.160	1.04	26.59	0.13
2-3	75	43.2	39.9	3.89	7.20	0.92	0.090	0.167	1.10	28.25	0.10
2-4	100	44.8	42.4	4.52	7.75	0.95	0.100	0.173	1.16	28.70	0.09

Note:  $f_{cu}$  is the cube compressive strength,  $f_c$  is axial compressive strength,  $f_{ts}$  is splitting tensile strength,  $f_f$  is flexural strength,  $f_c / f_{cu}$  is the ratio of compressive strength and compressive strength,  $f_{ts} / f_{cu}$  is tension compression's ratio, namely the ratio of splitting tensile strength and compressive strength,  $f_f / f_{cu}$  is the ratio of flexural strength and compressive strength, SFCR is the ratio of flexural strength and the square root of compressive strength,  $SFCR = f_f / f_{cu}^{1/2}$ ,  $E_c$  is elastic modulus,  $\nu$  is Poisson's ratio.

It can be found from Table 2 that the cube compressive strength of LCSARP increases with the incremental replacement rate of natural sand. Compared with all light concrete, the cube compressive strength increase by 11.7%, 17.6%, 20.7% and 25.1%, with the replacement rate of 25%, 50%, 75%, and 100%, respectively. The experiment shows that the compressive strength of all light concrete can be improved with shale pottery partly or completely replaced by nature sand. The main reason is that the average particle size of shale pottery is larger than natural sand. The smaller the replacement rate of natural sand is, the looser the skeleton structure of cement mortar is, and the lower the strength of the specimen is. When the replacement rate of natural sand is larger, the smaller the average particle size of fine aggregate is, the more the contact surface is, which can make a result that the cohesion between fine aggregate and cement mortar is enhanced, especially for natural sand and cement mortar, and the small particle size of natural sand reduces the probability of cracks.

The dimensionless of axial compressive strength of LCSARP has a linear relationship with the replacement rate  $\gamma$  of natural sand. According to the principle of least-squares method, the experimental data is fitted as followed:

$$f_c / f_{c,0} = 0.68\gamma + 1.09 \quad R^2 = 0.91 \quad (2)$$

Therefore, the compressive bearing capacity of LCSARP increases with the incremental replacement rate of natural sand.

The dimensionless of cube compressive strength of LCSARP has a linear relationship with the replacement rate  $\gamma$  of natural sand. According to the principle of least-squares method, the experimental data is fitted as followed:

$$f_{cu} / f_{cu,0} = 0.24\gamma + 1.03 \quad R^2 = 0.91 \quad (1)$$

where  $f_{cu,0}$  is the cube compressive strength of all light concrete.

The axial compressive strength of LCSARP increases with the incremental replacement rate of natural sand in Table 2. Compared with all light concrete, the axial compressive strength increase by 36.4%, 45.3%, 61.5%, and 71.7%, with the replacement rate of 25%, 50%, 75%, and 100%, respectively. The reason is the same as the cube compression.

where  $f_{c,0}$  is the axial compressive strength of all light concrete.

The splitting tensile strength of LCSARP increases with the incremental the replacement rate of natural sand in Table 2. Compared with all light concrete, the splitting tensile strength increase by 10.2%, 20.1%, 24.3%, and 44.4%, with the replacement rate of 25%,

50%, 75%, and 100%, respectively. There are many factors affecting the tensile splitting failure of LCSARP, such as the aggregate strength and void in the LCSARP. When replacement rate of natural sand is smaller, the ceramsite and shale pottery of lower strength account for a large percentage, which has a negative effect on the splitting tensile strength of LCSARP. With the incremental replacement rate of natural sand, the gaps between mortar and ceramsite can be more filled by nature sand, the compactness in the specimens is enhanced significantly, which can increase the splitting tensile strength of LCSARP gradually.

The dimensionless of tensile splitting strength of LCSARP has a linear relationship with the replacement rate  $\gamma$  of natural sand. According to the principle of least-squares method, the experimental data is fitted as followed:

$$f_{ts} / f_{ts,0} = 0.41\gamma + 0.99 \quad R^2 = 0.94 \quad (3)$$

where  $f_{ts,0}$  is the tensile splitting strength of the all light concrete.

It can be found from Table 2 that the flexural strength of LCSARP increases with the incremental replacement rate of natural sand. Compared with all light concrete, the flexural strength of LCSARP increase by 2.5%, 10.7%, 18%, and 27%, with the replacement rate of 25%, 50%, 75%, and 100%, respectively. The experiment shows that the flexural strength of all light concrete can be improved with shale pottery partly or completely replaced by nature sand. The main reason is that there are large gripping power between the natural sand of high strength and cement mortar, after the cementing force and mechanical interlocking in tension surface are well put to good use, the development of cracks is decreased. Natural sand and cement mortar complement each other, which is an effective way to improve the flexural strength of LCSARP.

The dimensionless of flexural strength of LCSARP has a linear relationship with the replacement rate  $\gamma$  of natural sand. According to the principle of least-squares method, the experimental data is fitted as followed:

$$f_f / f_{f,0} = 0.28\gamma + 0.98 \quad R^2 = 0.96 \quad (4)$$

where  $f_{f,0}$  is the flexural strength of the all light concrete.

### 4.3 Strength index conversion

Based on the results in the Table 2, it can be concluded that compared with the all light concrete, the  $f_c / f_{cu}$  increase 21.7%, 23.2%, 33.3%, and 37.7%,

with the replacement rate of 25%, 50%, 75%, and 100%, respectively.

It is shown in Figure 2 that the  $f_c / f_{cu}$  of LCSARP has a linear relationship with the replacement rate of natural sand  $\gamma$ . According to the principle of least-squares method, the experimental data is fitted as followed:

$$f_c / f_{cu} = 0.23\gamma + 0.73 \quad R^2 = 0.90 \quad (5)$$

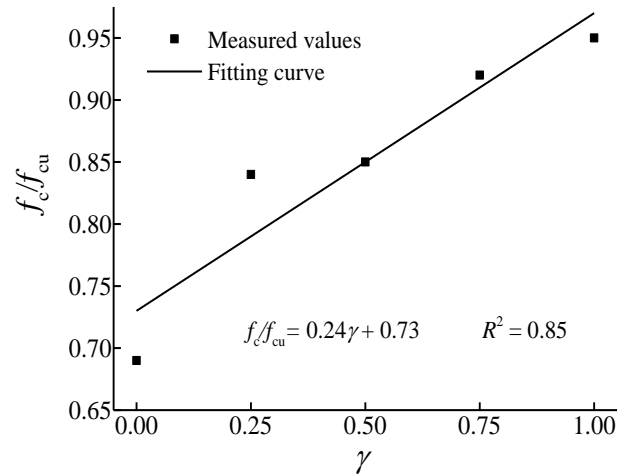


Figure 2. The relationship curve between  $f_c / f_{cu}$  and  $\gamma$

The tension and compression's ratio is one of the main indicators to reflect the brittleness of concrete. For concrete, the greater the tension and compression's ratio is, the smaller the brittleness is, and the greater the toughness is. In this experiment, the tensile and compression' ratio of LCSARP varied from 0.086 to 0.100, and increased generally with the incremental replacement rate of natural sand. Compared with all light concrete, the ratio of tensile and compression decreases little for the replacement rate at 25%, and increases by 2.3%, 3.4%, and 14.9%, with the replacement rate of 50 %, 75%, and 100%, respectively. When the replacement rate of natural sand is less than or equal to 50%, the cube compressive strength of LCSARP has grown at a much faster rate than splitting tensile strength. Therefore, tension and compression' ratio increases a little, which indicates the characteristics of large brittleness and little toughness for LCSARP. As the replacement rate of natural sand is greater than 50%, the tensile and compression' ratio has grown at a much faster rate, which indicates the characteristics of little brittleness and large toughness for LCSARP. A conclusion can be draw that shale pottery is replaced by a certain amount of natural sand, which can improve the brittleness of all light concrete, with the result that the LCSARP has the characteristics of large deformation capacity.

From Table 2, it can be found that the *SFCR* of LCSARP increases with the incremental replacement

rate of natural sand on the whole, and shows more obvious regularity compared with the  $f_{ts} / f_{cu}$ . Compared with all light concrete, the *SFCR* of LCSARP with 25% nature sand decreases little. As the replacement rate of natural sand is greater than 25%, the growth rate of flexural strength increases more rapidly than cube compressive strength, with the result that the *SFCR* increases with the incremental replacement rate. Compared with all light concrete, *SFCR* increases by 2.0%, 7.8%, and 13.7%, with replacement rate of 50%, 75%, and 100%, respectively.

It can be found that *SFCR* of LCSARP has a non-linear relationship with the replacement rate  $\gamma$  in Figure 3. According to the principle of least-squares method, the experimental data is fitted as followed:

$$SFCR = 0.22\gamma^2 - 0.061\gamma + 1.01 \quad R^2 = 0.93 \quad (6)$$

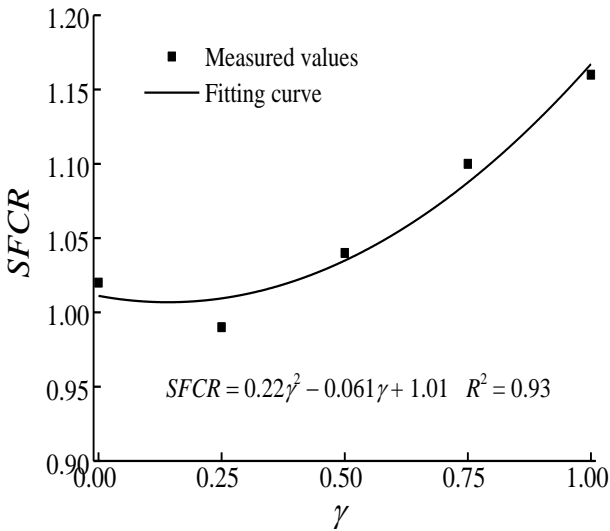
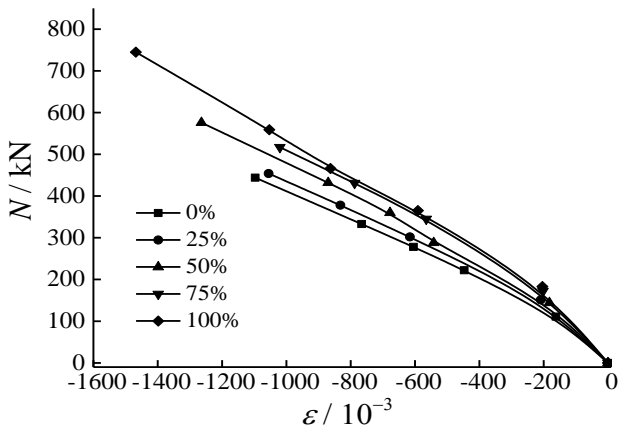


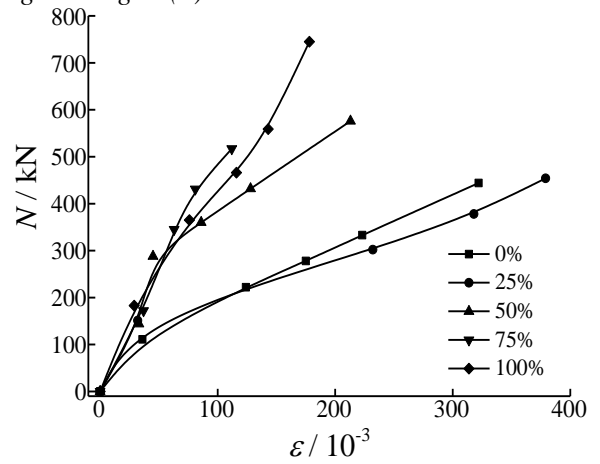
Figure 3. The relationship curve between *SFCR* and  $\gamma$

#### 4.4 Deformation properties

The load-strain curve was plotted in Figure 4, in which the Figures 4(a) and 4(b) presented the compressive strain in the axial direction and the tensile strain in the lateral direction, respectively.



a) Load-axial strain curve



b) Load-lateral strain curve

Figure 4. The relationship curve of load versus strain

From Figure 4, with the incremental replacement rate of natural sand, the slope increases gradually in the upward section of axial load-strain curve, which indicates the elastic modulus of LCSARP increases gradually. Due to the factor that lightweight aggregate distributed uniformly in specimen with has large elasticity modulus and rigidity in the initial elastic stage, which restrained strongly for the strain capacity of matrix, so both lateral deformation and axial deformation have a approximately linear relationship with the bearing capacity of specimen. As the axial strain further increased, the continuous formation of micro cracks caused lateral expansion gradually, so the lateral strain increased at a faster pace. As the load further increased, the lateral deformation exceeded the utmost tensile deformation of LCSARP, the adjacent cracks were penetrated, then the prism specimen split into a number of separate small prisms, which caused serious stress concentration and accelerated the failure of LCSARP.

From Table 2, it can be found that the elastic modulus of LCSARP increases gradually with the incremental replacement rate of natural sand. Compared with all light concrete, the elastic modulus of LCSARP increases by 0.5%, 20.5%, 28.1%, and 30.1%, with the replacement rate of 25%, 50%, 75%, and 100%, respectively. The main reason is that the elastic modulus of natural sand is larger than ceramsite and shale pottery, in which the elastic modulus is  $(0.50-3.00) \times 10^4$  MPa for ceramsite and shale pottery, but generally  $(2.79-4.76) \times 10^4$  MPa for nature sand. Therefore, the elastic modulus of cement mortar in LCSARP has been improved with the increase proportion of natural sand in specimen, and the overall elastic modulus of LCSARP increases.

Based on the results in the Table 2, it can be found that the Poisson's ratio of LCSARP changes from 0.09 to 0.28 in this experiment, and decreases gradually with the incremental replacement of natural sand. Compared with all light concrete, the Poisson's ratio

of LCSARP decreases by 35.7%, 53.6%, 64.3%, and 67.9%, with replacement rate of 25%, 50%, 75%, and 100%, respectively.

From Figure 5, it can be observed that the Poisson's ratio of LCSARP with low replacement rate of natural sand is almost equal to all light concrete when the stress ratio  $\sigma / f_c$  is small. For all light concrete, the Poisson's ratio increases in the order of magnitude 1:1 when the stress ratio is less than 0.2, and has larger variation when stress ratio is greater than 0.2. Meanwhile, an obvious law can be observed that no matter which stage of the stress ratio is, the Poisson's ratio of all light concrete is the largest among the five groups. Compared with all light concrete, the  $\sigma / f_c - \nu$  curve of LCSARP becomes steeper for the replacement rate at 25%. For replacement rate at 50%, when the stress ratio is greater than 0.2, the  $\sigma / f_c - \nu$  curve soars suddenly, and  $\nu$  does not change with the increase of stress ratio. The  $\sigma / f_c - \nu$  curves are approximately equal for the replacement rate of 75% and 100%, and  $\nu$  keeps a linear increase with the increase of  $\sigma / f_c$ , but it changes little after reaching  $0.6f_c$ .

Sun shows that the tension and compression's ratio of concrete is only determined by the Poisson's ratio under certain conditions, and the tension and compression's ratio of concrete indirectly reflects the distribution ratio between working energy and deformation energy under the compression state [30]. However, the Sun model is based on ordinary concrete. For further understanding and applying the law between tension and compression' ratio and Poisson's ratio for LCSARP, the Sun model was multiplied by a coefficient  $\alpha$ , and the expression was written as followed:

$$\frac{f_{ts}}{f_{cu}} = \alpha \frac{2\nu^2}{1+2\nu^2} \quad (7)$$

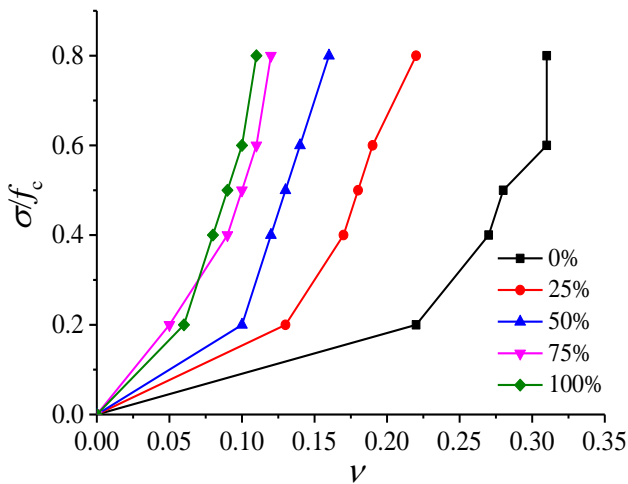


Figure 5. The curve of stress ratio versus Poisson's ratio

In this experience, the measured Poisson's ratio and tension and compression's ratio were substituted into formula (7) to obtain the value of  $\alpha$  under the replacement rate of 0%, 25%, 50%, 75%, and 100%, which were 0.64, 1.41, 2.72, 4.59, and 6.27 respectively. The relationship was analyzed and fitted between the replacement rate  $\gamma$  as the independent variable and the parameter  $\alpha$  as the dependent variable, as shown in Figure 4. The relevant data was fitted as followed:

$$\alpha = 5.78\gamma + 0.47 \quad R^2 = 0.99 \quad (8)$$

As seen in Figure 6, the value of  $\alpha$  could be obtained by substituting the  $\gamma$  of 0%, 25%, 50%, 75%, and 100% into formula (8), and subsequently by the formula (7), the  $f_{ts} / f_{cu}$  could be achieved.

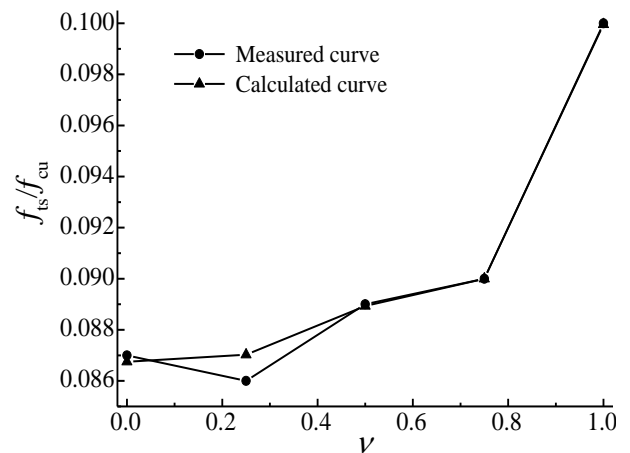


Figure 6. The comparison curves for  $f_{ts} / f_{cu}$  versus  $\nu$

The calculation curve of  $f_{ts} / f_{cu} - \nu$  was compared with the measured curve in Figure 6. It is found that the calculated curve for tension and compression's ratio correlates well to the experimentally measured result.

## 5 CONCLUSIONS

In this paper, sixty LCSARP test specimens were carried out experiment and analysis for strength and deformation performance, the conclusions are listed as followed:

(1) The failure mode of LCSARP is different from the ordinary concrete, and the LCSARP mainly shows cracking of lightweight aggregate. With the incremental replacement rate of natural sand, the failure mode is various under different experiment, such as fracture gradually, but without scattering under cube compressive, the failure changes from longitudinal failure to oblique shear failure under axial compressive, brittle failure occurs under splitting tensile, and

there is no vertical development and a standard mode for the main crack under flexural experiment.

(2) With the incremental replacement rate of natural sand, the mechanical properties of LCSARP show an increasing trend in performance in general, including cube compressive strength, axial compressive strength, splitting tensile strength, flexural strength,  $f_c / f_{cu}$ ,  $SFCR$ , and elastic modulus, while the reverse is true for the Poisson's ratio. In terms of LCSARP, the precise and applicable relationships for the mechanical property parameter as  $f_{cu}$ ,  $f_c$ , splitting tensile strength, flexural strength,  $f_c / f_{cu}$ , and  $SFCR$  at different replacement rates of natural sand are individually established by the regression analysis.

(3) Based on the introduced parameter in association with the replacement rate of natural sand, the curve equations between tension and compression's ratio and Poisson's ratio for LCSARP are established, and the calculated curve for tension and compression's ratio correlate well to the experimentally measured one.

## 6 ACKNOWLEDGEMENT

This work was financially supported by the National Natural Science Foundation of China (51774112; 51474188; 51074140), the Doctoral Fund of Henan Polytechnic University (B2015-67), Taihang Scholars Program, the Science and Technology Breakthrough Project of Henan Province (172102210285), and the Safe Production Project of Key Technology for Major Accident Prevention and Control (Henan-0006-2016AQ). All these are gratefully appreciated.

## 7 REFERENCE

- [1] Nadesan, M. S., Dinakar, P., "Structural concrete using sintered fly ash lightweight aggregate: A review". *Construction and Building Materials*, 154, 2017, pp.928-944.
- [2] Mydin, M. A. O., Wang, Y. C., "Thermal and mechanical properties of lightweight foamed concrete at elevated temperatures". *Magazine of Concrete Research*, 64(3), 2012, pp.213-224.
- [3] Yuwadee, Z., Ampol, W., Vanchai, S., "Use of lightweight aggregates in pervious concrete". *Construction and Building Materials*, 48, 2013, pp.585-591.
- [4] Waldron, C. J., Cousins, T. E., Nassar, A. J., "Demonstration of use of high-performance lightweight concrete in bridge superstructure in Virginia". *Journal of Performance of Constructed Facilities*, 19(2), 2005, pp.146-154.
- [5] Gao, X., Wu, X. W., Tian, J., "Structure of nonlinear finite element model of lightweight aggregate concrete shear wall and the factors affecting seismic performance". *Journal of Jilin University (Engineering and Technology Edition)*, 45(5), 2015, pp.1428-1435.
- [6] Zhang, B. Y., Poon, C. S., "Use of Furnace Bottom Ash for producing lightweight aggregate concrete with thermal insulation properties". *Journal of Cleaner Production*, 99, 2015, pp.94-100.
- [7] Anja, T., Lato, P., Vojislav, M., "Artificial fly ash based aggregates properties influence on lightweight concrete performances". *Ceramics International*, 41(2), 2015, pp.2714-2726.
- [8] Lim, E., Vinayagam, T., Wee, T. H., Tamilselvan, T., "Shear transfer in lightweight concrete". *Magazine of Concrete Research*, 63(6), 2011, pp.393-400.
- [9] Mo, K. H., Alengaram, U. J., Jumaat, M. Z., "A review on the use of agriculture waste material as lightweight aggregate for reinforced concrete structural members". *Advances in Materials Science and Engineering*, 63(6), 2014, pp.393-400.
- [10] Castro, J., Keiser, L., Golias, M., Weiss, J., "Absorption and desorption properties of fine lightweight aggregate for application to internally cured concrete mixtures". *Cement & Concrete Composites*, 33(10), 2011, pp.1001-1008.
- [11] Wang, G. M., Zhang, B., Shui, Z. H., "Experimental Study on the performance and microstructure of rubberized lightweight aggregate concrete". *Progress in Rubber Plastics and Recycling Technology*, 28(4), 2012, pp.147-156.
- [12] Wang, S. R., Xiao, H. G., Hagan, P., Zou, Z. S., "Mechanical behavior of fully-grouted bolt in jointed rocks subjected to double shear tests". *DYNA*, 92(3), 2017, pp.314-320.
- [13] Chen, W., Qian, J. S., Liu, J., Wang, H., Jia, X., "Preparation and properties of lightweight aggregate concrete by using higher water-cement ratio". *Journal of Building Materials*, 17(2), 2014, pp.298-335.
- [14] Li, J. J., Chen, Y. H., Wan, C. J., "A mix-design method for lightweight aggregate self-compacting concrete based on packing and mortar film thickness theories". *Construction and Building Materials*, 157, 2017, pp.621-634.
- [15] El-Hassan, H., Shao, Y. X., "Dynamic carbonation curing of fresh lightweight concrete". *Magazine of Concrete Research*, 66(14), 2014, pp.708-718.
- [16] Kim, K., Kang, S., "Manufacturing artificial lightweight aggregates using coal bottom ash and its application to the lightweight-concretes". *Journal of the Korean Crystal Growth and Crystal Technology*, 18(5), 2008, pp.211-216.
- [17] Ye, X. H., Xu, J. Y., Liu, J. L., "Dynamic performance of alumina bubble-basalt fiber lightweight aggregate concrete". *Journal of Vibration and Shock*, 34(16), 2015, pp.207-212.
- [18] Kockal, N. U., Ozturan, T., "Strength and elastic properties of structural lightweight concretes". *Materials and Design*, 32, 2011, pp.2396-2403.
- [19] Oktay, H., Yumrutas, R., Akpolat, A., "Mechanical and thermophysical properties of lightweight aggregate concretes". *Construction and Building Materials*, 96, 2015, pp.217-225.
- [20] Davraza, M., Ceylan, H., Kilincarslan, S., "Mechanical Performances of artificial aggregated lightweight concrete". *Acta Physica Polonica A*, 127(4), 2015, pp.1246-1250.
- [21] Li, B. X., Zhang, G. Z., Li, J. H. 2009. Durability of high performance light-weight aggregate concrete. *Journal of Building Materials* 12(5): 533-538.
- [22] Demirboga, R., Gul, R., "Durability of mineral admixed lightweight aggregate concrete". *Indian Journal of Engineering and Materials Sciences*, 11(3), 2004, pp.201-206.
- [23] Kockal, N. U., Ozturan, T., "Durability of lightweight concretes with lightweight fly ash aggregates". *Construction and Building Materials*, 25, 2011, pp.1430-1438.
- [24] Rossignolo, J. A., Agnesini, M. V. C., "Durability of polymer-modified lightweight aggregate concrete". *Cement & Concrete Composites*, 26, 2001, pp.375-380.
- [25] Wang, X. F., Fang, C., Kuang, W. Q., Li, D. W., Han, N. X., Xing, F., "Experimental investigation on the compressive strength and shrinkage of concrete with pre-wetted lightweight aggregates". *Construction and Building Materials*, 155, 2017, pp.867-879.
- [26] Yaseen, Z. M., Deo, R. C., Hilal, A., Abd, A. M., Bueno, L. C., Salcedo-Sanz, S., Nehdi, M. L., "Predicting

- compressive strength of lightweight foamed concrete using extreme learning machine model". *Advances in Engineering Software*, 115, 2018, pp.112-125.
- [27] Qian, W., Fan, C. G., Ran, S. L., Li, J. M., Guo, W. J., "Preparation and performance of specified density concrete of pottery sand made from fly ash". *Journal of Anhui University of Technology (Natural Science)*, 29(2), 2012, pp.157-161.
- [28] Ministry of Housing and Urban-Rural Development of the People's Republic of China, Standard for test method of performance on ordinary fresh concrete (GB/T 50080-2016). Beijing, China, 2016.
- [29] Ministry of Housing and Urban-Rural Development of the People's Republic of China, Standard for test method of mechanical properties on ordinary concrete (GB/T 50081-2002). Beijing, China, 2003.
- [30] Sun, N. P., "Research on tension and compression's ratio of concrete". *Building Science*, 30(7), 2014, pp.19-22.